Effect of antecedent rainfall patterns on rainfall-induced slope failure

Rahimi, Arezoo; Rahardjo, Harianto; Leong, Eng Choon

2011

Rahimi, A., Rahardjo, H., and Leong, E. C. (2011). Effect of Antecedent Rainfall Patterns on Rainfall Induced Slope Failure. Journal of Geotechnical and Geoenvironmental Engineering, 137(5), 483-491.

https://hdl.handle.net/10356/101531

https://doi.org/10.1061/(ASCE)GT.1943-5606.0000451

Effect of Antecedent Rainfall Patterns on Rainfall-Induced Slope Failure

Arezoo Rahimi[1], Harianto Rahardjo[2] and Eng-Choon Leong[3]

Abstract:

Rainfall-induced slope failure occurs in many parts of the world especially in the tropics. Many rainfall-induced slope failures have been attributed to antecedent rainfalls. Although, it has been identified as a cause of rainfall-induced slope failure, the pattern or distribution of the antecedent rainfall has not received adequate attention. In this study, parametric studies were performed using three typical rainfall patterns identified by analysis of available rainfall data of Singapore and two different soil types to represent high and low conductivity residual soils of Singapore. Antecedent rainfall patterns were applied on soil slopes and a transient seepage analysis was conducted. The computed pore-water pressures were used in stability analyses to calculate factor of safety of the slope. Results indicated that antecedent rainfall affected stability of both high conductivity (HC) and low conductivity (LC) soil slopes. However, it affected the stability of LC soil slope more significantly than HC soil slope. Patterns of antecedent rainfall controlled the rate of decrease in factor of safety, the time corresponding to $F_{s(min)}$ and the value of $F_{s(min)}$. Delayed rainfall pattern resulted in the lowest minimum factor of safety, $F_{s(min)}$, for HC soil slope and advanced rainfall pattern resulted in the lowest $F_{s(min)}$ for LC soil slope.

[1] Project Officer, School of Civil & Environmental Engineering, Nanyang Technological University, Block N1, B4c-10, Nanyang Avenue, Singapore 639798

[2] Professor, School of Civil & Environmental Engineering, Nanyang Technological University, Block N1, 01b-36, Nanyang Avenue, Singapore 639798

[3] Associate Professor, School of Civil & Environmental Engineering, Nanyang Technological University, Block N1, 01c-80, Nanyang Avenue, Singapore 639798

Keywords: Rainfall pattern**,** Antecedent rainfall, Rainfall-induced slope failure, Slope stability, Factor of safety

Introduction

Slope failure is a natural disaster that occurs in many parts of the world. Rainfall is the most recognized triggering factor for this disaster, especially in tropical regions with hot and humid climatic conditions (Brand 1984; McDougall et al. 1999; Tsaparas et al. 2002; Collins et al. 2004; Chen et al. 2004; Tohari et al. 2007; Tsai et al. 2008; Frattini et al. 2009). Tropical climate results in formation of residual soils which usually exist in unsaturated conditions (Rahardjo et al., 1995). Rainwater infiltrates into the unsaturated zone of soil slope, decreases matric suction and consequently shear strength of soil, causing slope failures (Yoshida et al. 1991; Fourie 1996; Au 1998; Crosta 2001; Kim et al. 2004; Rahardjo et al. 2005; Calvello and Cascini 2007). Although there are many relations between rainfall and slope failures, there have been some debates as to the relative role of antecedent rainfall. Antecedent rainfall is the rain that falls in the days immediately preceding a landslide event (Au, 1998; Rahardjo et al., 2001; Cai and Ugai, 2004). Guzzetti et al. (2007) reviewed rainfall thresholds for initiation of landslides and found that many researchers in different parts of the world related landslides to antecedent rainfall, but with different durations, from 1 day to 120 days. However, the effect of antecedent rainfall is still controversial. Brand (1984) concluded that localised short-duration rainfalls of high intensity induced the majority of landslides in Hong Kong. Brand (1992) also concluded that due to the high conductivity of Hong Kong soils, the effect of antecedent rainfall on rainfall-induced slope failure was not significant. Studies in Italy showed that antecedent rainfall did not have a relation with landslides (Aleotti, 2004). Pitts (1984) concluded that antecedent rainfall was not a significant factor for slope failures in Singapore. Tan et al. (1987) found that antecedent rainfall could be

significant in inducing slope instability in Singapore. Bukit Batok landslide (Wei et al., 1991) was an evidence that showed the effect of antecedent rainfall in Singapore. The failure occurred after a period of heavy rainfall, although no rainfall occurred at the time of failure. Rahardjo et al. (2008) studied the slope responses (i.e., pore-water pressure distribution) to rainfall events through comprehensive instrumentation of four slopes in Singapore and concluded that 5-day antecedent rainfall could affect stability of slopes in Singapore. It was concluded that the role of antecedent rainfall on rainfall-induced slope failure greatly depends on permeability of soil.

Although, it has been identified that antecedent rainfall resulted in slope failure, the effects of pattern or distribution of antecedent rainfall on rainfall-induced slope failures have not received adequate attention. Ng et al. (2001) studied the effect of rainfall pattern on pore-water pressure changes in slope and concluded that rainfall patterns had a significant effect on pore-water pressure changes. However, stability of slope was not investigated in this work. Therefore, the effect of antecedent rainfall pattern on rainfall-induced slope failure needs further investigation.

Tsaparas et al. (2002) studied the factors controlling rainfall-induced slope failure including antecedent rainfall. In this study, a fixed amount of rainfall was considered and distributed uniformly for different time periods in order to obtain different antecedent rainfall intensities. However, the uniform rainfall distribution may not truly represent the actual rainfall patterns. Therefore, there is a need to investigate the actual rainfall data and their typical patterns that closely represent the field condition.

The study presented in this paper focused on the effect of antecedent rainfall pattern on stability of slopes. Actual rainfall data from various parts of Singapore were analyzed to identify repeatable rainfall patterns. The identified rainfall patterns were then applied to two different soil types which represent high and low conductivity residual soils of

Singapore. A major rainfall event based on actual rainfall data was then applied to slopes right after the application of the antecedent rainfall. In order to study stability of slope subjected to various antecedent rainfall patterns, two analyses, seepage and stability were performed. Transient seepage analysis was conducted to compute the pore-water pressures. The computed pore-water pressures were then used to calculate factor of safety of slope during rainfall.

Theoretical consideration

The seepage analysis was performed using SEEP/W (Geo-slope International, 2004a). The following water-flow governing equation for solving transient and two dimensional seepage analyses was used in this study:

$$m_w^2 \gamma_w \frac{\partial h_w}{\partial t} = \frac{\partial}{\partial x}\left(-k_{wx}\frac{\partial h_w}{\partial x}\right) + \frac{\partial}{\partial y}\left(-k_{wy}\frac{\partial h_w}{\partial y}\right) + q \quad (1)$$

where m_w^2=slope of soil-water characteristic curve; γ_w= unit weight of water; h_w= hydraulic head or total head; t = time; k_{wx}= coefficient of permeability with respect to water as a function of matric suction in x-direction; k_{wy}= coefficient of permeability with respect to water as a function of matric suction in y-direction; and q = applied flux at the boundary.

Slope stability analysis was carried out in this study by considering shear strength contribution from negative pore-water pressure or matric suction in unsaturated soil using the Fredlund et al. (1978) equation:

$$\tau = c' + (\sigma_n - u_a)tan\phi' + (u_a - u_w)tan\phi^b \quad (2)$$

where τ = shear strength of unsaturated soil; c' = effective cohesion; $(\sigma_n - u_a)$ = net normal stress; σ_n= total normal stress; u_a = pore-air pressure; ϕ' = effective angle of internal friction; $(u_a - u_w)$ = matric suction; u_w = pore-water pressure; and ϕ^b = angle indicating the rate of change in shear strength relative to a change in matric suction.

Bishop's simplified method was used to compute factor of safety, F_s, of slopes using Slope/W (Geo-slope International, 2004b).

Numerical model

Slope geometry

Fig. 1 shows slope geometry and boundary conditions used in this study. One slope angle (α=30˚) and one slope height (H_s=15m) based on a typical slope geometry in Singapore (Toll et al., 1999) was examined in this study. The depth of water table, H_w, was defined as a distance from the toe of slope to the water table. The initial depth of water table, H_w, was selected to be 2 m below the ground surface based on typical ground water condition in Singapore.

The boundary conditions used for the transient seepage analysis are shown in Fig. 1. A boundary flux, q, equal to rainfall intensity, I_r, was applied to the surface of the slope. The nodal flux, Q, equal to zero was applied along the sides of the slope above the water table and along the bottom of the slope to simulate no flow zone. A boundary condition equal to total head, h_w, was applied along the sides of the slope below the water table. To achieve an initial condition for the homogenous soil slope the following procedure was conducted.

Initial condition

First, a very small quantity of rainfall, q was applied to the surface of slope for a long duration of time in order to achieve a target depth of water table, H_w at the toe of slope (i.e., H_w = 2 m) and at an inclination of 5˚ with respect to the horizon (refer to Fig. 1). The pore-water pressure distributions above the water table were plotted for all time steps at selected sections, section x-x and section y-y as shown in Fig. 1. This was done to ensure the pore-water pressure distributions were stable and represented a steady state condition. Even though slopes with two different soil types reached the same target depth of water

table (i.e., H_w=2 meters), the response of each soil type to the applied boundary flux, q, was different. In fact, distributions of the pore-water pressure above water table were different for different soil types. Therefore, the initial factors of safety, $F_{s(ini)}$, of slopes were different. To have comparable data, the normalized factor of safety, F_{sn} defined as the ratio of factor of safety at each time step to the initial value of factor of safety, was used to compare the results.

Soil properties

To study the effect of antecedent rainfall patterns on stability of slopes, two types of soil were considered. One soil type was selected to represent high conductivity residual soils of Singapore and was named HC soil. The other soil type was selected to represent low conductivity residual soils and was named LC soil. Fig. 2 shows SWCC and unsaturated permeability function, k_w, of HC and LC soils. Fredlund and Xing (1994) equation with a correction factor, $C(\psi) = 1$ as recommended by Leong and Rahardjo (1997) was used to describe the SWCC of soils in this study.

Saturated coefficient of permeability of HC soil, k_s, was equal to 10^{-4} m/s and soil-water characteristic curve (SWCC) parameters of the soil were a=10 kPa, m=0.5 and n=1. Saturated coefficient of permeability of LC soil was equal to 10^{-6} m/s. Soil-water characteristic curve parameters of LC soil were a=300 kPa, m=1 and n=1. For computation of unsaturated permeability function, k_w, from SWCC the indirect procedure described in Fredlund and Rahardjo (1993) was used.

Shear strength properties of the soils used in the study were selected based on typical shear strength properties of soils in Singapore (Rahardjo et al., 2007). An effective cohesion, c′=10 kPa, effective angle of internal friction, ϕ'=26˚, angle indicating the rate of change in shear strength relative to a change in matric suction, ϕ^b=26˚, and unit weight of soil, γ=20 kN/m^3, were used in the slope stability analyses. To ensure that

changes in stability of the slope were only due to pore-water pressure (or matric suction) changes in the soil, shear strength parameters of the soils were kept constant for all cases.

Designing rainfall patterns and major rainfall

Three typical rainfall patterns were selected by analyses of available rainfall data of Singapore. Data were collected from online monitoring of rainfall at different locations in Singapore. Duration associated with the different rainfall patterns was selected to represent antecedent rainfalls in Singapore. It was found that 3-day, 4-day and 5-day antecedent rainfall were the most repeated durations in the collected rainfall data. Rahardjo et al. (2008) found that a 5-day antecedent rainfall caused the worst pore-water pressure profiles in slopes in Singapore. Therefore, in this study, 5-day (i.e., 120 h) was selected to represent the duration of the rainfall patterns. The 5-day duration was divided into equal time intervals to distribute the antecedent rainfalls. A long duration time interval would result in few time intervals with very low rainfall intensities which caused difficulties in distinguishing different rainfall patterns. On the other hand, a short duration time interval would result in scattered rainfall patterns that are difficult to categorize. Based on these criteria, the time interval for distributing the rainfall was selected to be 8 hours. Each 5-day antecedent rainfall comprised 15 time intervals (i.e., 120 hours / 8 hours). Ng (2001) selected 14 hours time interval to distribute the antecedent rainfall. Procedure to recognize these patterns is described here as an example for rainfall data at Ulu Pandan Sewage Treatment Works, in December 2006. The month of December comprises 31 days. Since each day is 24 hours; therefore, December 2006 comprised 744 hourly rainfall data. The total amount of rainfall was computed as follows:

$$rd_1 + rd_2 + \cdots + rd_{744} = 675.3\ mm \quad (4)$$

where rd = rainfall data and the subscript is time (h), rd_1 means rainfall data of first hour of the month. All 8 hourly rainfall data were summed continuously as follows:

$$rd_1 + rd_2 + \cdots + rd_8 = R_1\ [mm]$$

$$rd_9 + rd_{10} + \cdots + rd_{16} = R_2\ [mm]$$

$$\ldots\ldots\ldots\ldots\ldots\ldots\ldots\ldots\ldots\ldots\ldots\ldots\ldots\ldots\ [mm] \quad (5)$$

$$\ldots\ldots\ldots\ldots\ldots\ldots\ldots\ldots\ldots\ldots\ldots\ldots\ldots\ldots\ [mm]$$

$$rd_{737} + rd_{738} + \cdots + rd_{744} = R_{93}\ [mm]$$

Each equation represents the amount of rainfall data for one time interval (i.e., R_1.is the rain that falls within the first 8 hours of the month). To obtain one antecedent rainfall, 15 time intervals were needed. The rainfall data of these 15 running, 8-hour, time intervals were summed as follows:

$$R_1 + R_2 + \cdots + R_{15} = T_1\ [mm]$$

$$R_2 + R_3 + \cdots + R_{16} = T_2\ [mm]$$

$$\ldots\ldots\ldots\ldots\ldots\ldots\ldots\ldots\ldots\ldots\ldots\ldots\ldots\ [mm] \quad (6)$$

$$\ldots\ldots\ldots\ldots\ldots\ldots\ldots\ldots\ldots\ldots\ldots\ldots\ldots\ [mm]$$

$$R_{79} + R_{80} + \cdots + R_{93} = T_{79}\ [mm]$$

Each equation represented a 5-day antecedent rainfall. For each of the above equations, the percentage of the rain that fell in each time interval (i.e., R_1, $R_{2...}$ R_{15}) was calculated out of the total rainfall that fell in one antecedent rainfall (i.e., T_1). In order to observe the pattern of the antecedent rainfall, each of the above equations was plotted in such a way that x-axis was the time interval and y-axis was the calculated percentage of rainfall. Each of the plots shows a unique rainfall pattern. In general, the different patterns could be categorized into three different groups as shown in Fig. 3. For instance, in Fig. 3a, rainfall started at low intensity and gradually increased at the end. Fig. 3b shows rainfall started at low intensity at the beginning of rainfall duration. It increased gradually at the middle and then decreased again at the end of rainfall. Fig. 3c shows rainfall started at high intensity at the beginning and then decreased gradually at the end of rainfall duration. These three

patterns were selected among all the recognized rainfall patterns and then idealized as shown in the figure. The maximum continuous 5-day rainfall was calculated from the available rainfall data and was found to be 450 mm. This value, 450 mm rainfall was then distributed based on the idealized rainfall patterns. It was multiplied by the idealized rainfall percentage for each time interval, for the three recognized rainfall patterns. In order to obtain rainfall intensity, the total rainfall in each time interval was divided by 8 hours. Fig. 4 shows finalized antecedent rainfall patterns used in this study. First rainfall pattern was named delayed rainfall pattern (Fig. 4a). Second rainfall pattern which is similar to a normal distribution was named normal pattern (Fig. 4b). Third rainfall pattern was named advanced rainfall pattern (Fig. 4c).

A major rainfall was also considered in the analysis. Duration of major rainfall was selected to be 8 hours (i.e., same as rainfall pattern intervals). A maximum of 8 continuous hours of rainfall of 180 mm was obtained from the available rainfall data. This value was divided by 8 hours to calculate the major rainfall intensity of 22.5 mm/h. Public Utilities and Board of Singapore also uses this rainfall intensity for drainage designs in Singapore (PUB, 2000).

Results and discussion

Three typical antecedent rainfall patterns, namely delayed, normal and advanced were used to investigate the effect of antecedent rainfall patterns on slope stability. The antecedent rainfall patterns were applied to the homogenous soil slopes of two different soil types, HC and LC. A major rainfall with an intensity of 22.5 mm/h for a duration of 8 hours was applied to the slopes right after the application of antecedent rainfall patterns. The stability of the slopes was assessed through factor of safety, F_s, calculation and the results are presented below.

Effect of antecedent rainfall patterns on stability of slope

Fig. 5 provides the results obtained from the numerical modeling of HC and LC slopes under delayed, normal and advanced rainfall patterns. The results are presented in factor of safety, F_s, versus time, t. Fig. 5a shows the results for HC soil slope and Fig. 5b shows the results for LC soil slope.

Fig. 5a shows that the rate of decrease in factor of safety versus time was faster for the advanced pattern followed by the normal and delayed patterns. It also shows that the minimum factor of safety, $F_{s(min)}$ occurred at 56, 88 and 120 hours for the advanced, normal and delayed patterns, respectively. The lowest $F_{s(min)}$ corresponded to the delayed pattern which was equal to 1.48, followed by the normal ($F_{s(min)}$=1.51) and the advanced ($F_{s(min)}$=1.53) patterns. However, the difference in $F_{s(min)}$ for all the rainfall patterns was not significant. The rate of recovery in the factor of safety versus time was fastest for the delayed pattern followed by the normal and advanced patterns.

Fig. 5b shows that rate of decrease in the factor of safety versus time was fastest for the advanced pattern followed by the normal and delayed patterns. It also shows that the minimum factor of safety, $F_{s(min)}$ occurred at 96, 112 and 120 hours for the advanced, normal and delayed patterns, respectively. The value of $F_{s(min)}$ corresponding to the advanced, normal and delayed pattern was equal to 1.001, 1.004 and 1.083. The lowest $F_{s(min)}$ corresponded to the advanced rainfall pattern. Even though, the lowest $F_{s(min)}$ corresponded to the advanced rainfall pattern, the magnitude of $F_{s(min)}$ was more or less the same for all the rainfall patterns; however, they occurred at different times. As it can be seen from Fig. 5b, the rate of recovery in factor of safety was slower for the delayed pattern in comparison with the normal and advanced patterns.

Comparison between high and low conductivity soils

As shown in Fig.5c, the rainfall patterns affected the rate of reduction in F_s and the time corresponding to $F_{s(min)}$ for both HC and LC soil slopes. The F_s of HC soil slope decreased by 10-13 percents from its initial value and the F_s of LC soil slope decreased to 40-45 percents of its initial value. Fig. 6 shows pore-water pressure distributions at the crest (section x-x) and toe (section y-y) of HC soil slope during the application of antecedent rainfall of different patterns. Fig. 6a shows pore-water pressure distribution for the delayed rainfall pattern. As shown in the figure, the pore-water pressure near ground surface at the crest increased gradually from -38.5 kPa at t = 0 h (beginning of the rainfall) to -8.5 kPa at t = 120 h (at the end of rainfall corresponding to $F_{s(min)}$). In other words, the matric suction of the soil decreased by 30 kPa. Fig. 6a also shows that the pore-water pressure increased from -18.5 kPa at t = 0 to -7.1 kPa at t = 120 h near the ground surface at the toe of slope. The reduction in matric suction was 11.4 kPa. The maximum reduction in matric suction of the slope which was at the end of rainfall (i.e., t = 120) resulted in $F_{s(min)}$. This reduction in matric suction of HC soil slope corresponded to the first 7 m depth below the slope surface at the crest. The figure shows that the position of water table did not change significantly (i.e., increased from 28 m to 28.83 m at the toe of slope). This observation indicated that the reduction in matric suction of the slope was mainly caused by infiltration of rainwater rather than by rising of water table.

Fig. 6b shows pore-water pressure distribution associated with the normal rainfall pattern. As shown in the figure, the pore-water pressure near the ground surface increased from its minimum value of -38.5 kPa at t = 0 h (at the beginning of rainfall) to its maximum value of -9.85 kPa at t = 88 h which correspoded to $F_{s(min)}$ of the slope. The increase in pore-water pressure was 74 percent. The pore-water pressures started to decrease towards negative value from t = 88 h although rainfall continued until t = 120 h

(end of the rainfall). This behavior was also observed at the toe of slope. This can be attributed to the fact that as the rainwater infiltrated into the unsaturated zone of slope, the pore-water pressures increased. When the rainwater percolated down in the slope, the matric suction decreased at deeper depths and the depth of wetting front increased. When the infiltrated rainwater became less than the percolated rainwater, pore-water pressures started to recover. As the pore-water pressures decreased towards negative value, the shear strength of soil increased and consequently the factor of safety of slope started to increase.

Fig. 6c shows pore-water pressure distributions associated with the advanced rainfall pattern. As shown in the figure, the pore-water pressure at the ground surface at the crest of slope increased from -38.5 kPa at t = 0 h (at the begining of rainfall) to -12.5 kPa at t = 56 h. The increase in pore-water pressure was about 68 percents. The pore-water pressures started to decrease from t = 64 h although rainfall continued until t = 120 h (end of the rainfall). This behavior was also observed at the toe of slope for the same reason for the normal rainfall pattern.

Fig. 7a shows infiltrated rainwater into the slope versus time for all the rainfall patterns at the crest of the HC soil slope. As indicated in Fig. 4 the maximum rainfall intensity for all the rainfall patterns was 8.5 mm/h which was 2.36 percent of k_s of HC soil slope (i.e., k_s = 360 mm/h). As a result, all the rainwater infiltrated into the slope (i.e., crest and toe) as indicated in Fig. 7a. This can be attributed to the fact that rainfall intensity at all time was much smaller than the saturated coefficient of permeability, k_s, of HC soil slope. Although all the rainwater infiltrated into the soil under all the three rainfall patterns, the amount of infiltrated rainwater at each time step was different and it controlled the value of $F_{s(min)}$. For HC soil, the advanced rainfall pattern which had the highest amount of infiltrated rainwater in the early stage, was the first antecedent rainfall pattern to reach

$F_{s(min)}$ (i.e., t = 56 hours). The delayed rainfall pattern which had the highest cumulative infiltrated rainwater (i.e., 440 mm) resulted in the lowest $F_{s(min)}$ (i.e., $F_{s(min)}$= 1.48). The higher the amount of infiltrated rainwater, the lower the value of $F_{s(min)}$.

Fig. 8 shows pore-water pressure distributions at the crest (section x-x) and toe (section y-y) of LC soil slopes during the application of antecedent rainfall of different patterns. Fig. 8a shows pore-water pressure distribution for the delayed rainfall pattern. As shown in the figure, the pore-water pressure near the ground surface at the crest of slope increased from -141 kPa at t = 0 h (beginning of the rainfall) to 0 kPa at t = 120 h. The figure also shows that the pore-water pressure at the toe of slope increased from -19.4 kPa at t = 0 h to 0 kPa at t = 32 h. It can be seen that the water table rose to the ground surface at the toe of slope (i.e., at t = 32 h). It also rose to the middle of the slope at t = 120 hours. Therefore, the reduction in matric suction was attributed to both the rainwater infiltration and the rising of water table.

Fig. 8b shows pore-water pressure distributions for the normal rainfall pattern. As shown in the figure, the pore-water pressure near the ground surface at the crest of slope increased from -141 kPa at t = 0 h (beginning of the rainfall) to 0 kPa at t = 64 h. However, the water table rose to its highest position at t = 112 hours which corresponded to $F_{s(min)}$ of the slope. The figure also shows that the pore-water pressure at the toe of slope increased from -19.4 kPa at t = 0 h to 0 kPa at t = 24 h. It can be seen that the water table rose to the ground surface at the toe of slope (i.e., at t = 32 h). It can be noted that the reduction in matric suction of the slope was mostly attributed to the rising of water table. The same behavior was also observed for the advanced rainfall pattern (see Fig. 8c).

Fig. 7b shows infiltrated rainwater into the slope versus time for all the rainfall patterns at the crest of the LC soil slope. As shown in the figure, the changes in the rate of

rainwater infiltration into the soil follow the same pattern as the changes in the rate of rainfall for all the rainfall patterns. However, for the normal rainfall pattern, the amount of rainwater infiltration was less than the amount of rainfall from t = 56 h to t = 88 h. This behavior could be attributed to the capacity of the LC soil slope (i.e., k_s= 3.6 mm/h) which was smaller than the rainfall intensity in some stages of the application of rainfall. This behavior was also observed for the delayed pattern from t = 88 h to t = 120 h (see Fig. 7b). As it can be seen from the figure, the advanced rainfall pattern had the highest amount of infiltrated rainwater during its application on the LC soil slope and was the first antecedent rainfall pattern to reach $F_{s(min)}$. In addition, it resulted in the lowest $F_{s(min)}$.

It can be noted that the delayed rainfall pattern resulted in the lowest $F_{s(min)}$ for HC soil, while the advanced rainfall pattern resulted in the lowest $F_{s(min)}$ for LC soil. On the other hand, the advanced rainfall pattern was the first antecedent rainfall pattern to reach the $F_{s(min)}$ for both HC and LC soil slopes.

When the infiltrated rainwater became less than the percolated rainwater, pore-water pressures in the slope and subsequently the factor of safety of the slope started to recover for all rainfall patterns and soil types. It can be noted that the pattern of rainfall affects the trend of the pore-water pressure changes in the slope and infiltration characteristics into the slope, especially near the ground surface. As a result, the rainfall pattern also controls the factor of safety variation of the slope during rainfall.

Effect of major rainfall with different initial conditions on stability of slope

Major rainfall was applied to the slopes right after the application of the antecedent rainfall. It was also applied to the slopes without any antecedent rainfall (i.e., no rainfall before the major rainfall was applied). Due to the various antecedent rainfall patterns applied to the slope, the initial conditions (i.e., pore-water pressure distributions) of the

different slopes were different at the start of the major rainfall. This means that the antecedent rainfall patterns changed the pore-water pressure distributions in the slope prior to the major rainfall.

Fig. 9 shows pore-water pressure distributions for HC and LC soil slopes at the end of antecedent rainfall and for the case without any antecedent rainfall.

Fig. 9a shows that the antecedent rainfall, with the delayed, normal and advanced patterns changed the initial conditions for HC soil slope. As shown in the figure, the delayed rainfall pattern caused the worst initial condition. The worst initial condition means that the pore-water pressures profiles had the highest value at the crest and toe of the slope, which in turn caused the lowest factor of safety. The pore-water pressure caused by the delayed rainfall pattern near the ground surface at the crest of slope was -8.4 kPa. This value was -22.1 kPa, -24.6 kPa and -38.4 kPa for the normal and advanced patterns and no antecedent rainfall condition, respectively.

Fig. 9b shows the initial conditions caused by the antecedent rainfall patterns for LC soil slope. As shown in the figure, both normal and advanced rainfall patterns resulted in the same initial condition. The matric suction near the ground surface was -30 kPa for both of the normal and advanced rainfall patterns. This value was 0 kPa for the delayed rainfall pattern and it was -141 kPa for the case with no antecedent rainfall.

Fig. 10 provides the results of the numerical analyses of HC and LC soil slopes with a major rainfall of 22.5 mm/h for 8 hours. Fig. 10a shows the results for HC soil slope. As shown in the figure, the reduction in factor of safety due to the major rainfall was the same for all the initial conditions. For instance the major rainfall decreased the factor of safety from 1.48 to 1.39 for the initial condition generated by the delayed rainfall pattern. The percentage of the reduction was about 6 percent. This percentage was observed for the normal and advanced rainfall patterns. In the case of major rainfall (22.5 mm/h)

without any antecedent rainfall, the factor of safety decreased from 1.69 to 1.61. The percentage of the reduction was about 5 percent. This behavior shows that the major rainfall had the same effect on all the cases with and without antecedent rainfalls for HC soil slope. However, the role of antecedent rainfall can be observed in the initial factor of safety. For example the initial factor of safety at the beginning of major rainfall was 1.70 for the case without antecedent rainfall and was 1.48 for the delayed rainfall pattern. The initial factor of safety generated by the delayed rainfall pattern, 1.48, was about 87 percent of its initial value (i.e., 1.70). As a result of both the antecedent and major rainfalls, the factor of safety of the soil slope was decreased to 82, 87 and 87.5 percent of its initial value for the delayed, normal and advanced patterns, respectively. Therefore, the delayed rainfall pattern had the worst effect on the stability of HC soil slope.

Fig. 10b provides the results for LC soil type. As shown in the figure, the factor of safety at the end of application of antecedent rainfalls was approximately the same (i.e., $F_{s(t=120\ h)}$=1.083 for the delayed, $F_{s(t=120\ h)}$=1.024 for the normal and the advanced rainfall patterns). As it can be seen from the figure, for the initial condition resulting from the normal and advanced rainfall patterns, the major rainfall decreased the factor of safety of LC soil slope from 1.024 to a value less than one (i.e., 0.904) which reflected the unstable condition or failure of the slope. For the initial condition resulting from the delayed rainfall, the major rainfall decreased the factor of safety of the LC soil slope from 1.08 to 1.01 which was about 7 percent. The reduction in the factor of safety caused by the major rainfall for the initial condition resulting from the normal and advanced rainfall patterns was about 12 percent. As the infiltrated rainwater from the normal and advanced antecedent rainfall patterns was more than that of the delayed antecedent rainfall pattern, the reduction in factor of safety caused by the normal and advanced rainfall patterns was more than that of the delayed rainfall pattern.

In the case of major rainfall without any antecedent rainfall, the factor of safety of LC soil slope decreased to 1.62 from its initial $F_{s(ini)}$ (=1.82). The percentage of reduction was about 11 percent. The overall reduction in the factor of safety (i.e., antecedent rainfall patterns and major rainfall) for LC soil slope was about 50 percent for the normal and advanced rainfall patterns and 44.5 percent for the delayed rainfall pattern.

The major rainfall affected the stability of LC soil slope more significantly than the stability of HC soil slope in the case without antecedent rainfall. The reason was due to the fact that the major rainfall was 6.25 of k_s (saturated coefficient of permeability) for LC soil, causing F_s to decrease to 89 percent of its initial value. On the other hand, the major rainfall was 0.0625 of k_s (saturated coefficient of permeability) for HC soil, causing F_s to decrease to 95 percent of its initial value. Rahardjo et al. (2007) also concluded that for low conductivity soils ($k_s \leq 10^{-6}$ m/s), short duration rainfalls with intensity greater than $1k_s$ could bring the slope to its lowest F_s. While for high conductivity soil ($k_s \geq 10^{-4}$ m/s), a high rainfall intensity was needed to destabilize the slope.

It can be noted that the effect of antecedent rainfall patterns prior to the occurrence of major rainfall played a major role in stability assessment of HC and LC soil slopes. However, its effect is more significant in stability assessment of LC soil slopes.

Conclusions

Based on this study on the effect of antecedent rainfall patterns on slope stability, the following conclusions can be made:

Antecedent rainfall affected stability of both HC and LC soil slopes, by lowering the factor of safety of the slope prior to the occurrence of a major rainfall. The patterns of antecedent rainfall controlled the rate of decrease in factor of safety, the time corresponded to the minimum factor of safety, $F_{s(min)}$ and the value of $F_{s(min)}$. The rate of decrease in factor of safety was faster for the advanced rainfall pattern followed by the

normal and delayed rainfall patterns.

The value of $F_{s(min)}$ was controlled by the amount of infiltrated rainwater into the unsaturated zone of the slope. The higher the amount of infiltrated rainwater, the lower the $F_{s(min)}$ of the slope. For HC soil slope, the delayed rainfall pattern resulted in the lowest minimum factor of safety, $F_{s(min)}$ because the amount of infiltrated rainwater was the highest among all the antecedent rainfall patterns. For LC soil slope, the advanced rainfall pattern resulted in the lowest, $F_{s(min)}$ because the amount of infiltrated rainfall was the highest among all the antecedent rainfall patterns.

Antecedent rainfalls affected the stability of LC soil slope more significantly than HC soil slope. Antecedent rainfalls could cause up to 45 percent reduction in the factor of safety of LC soil slope and up to 13 percent reduction in the factor of safety of HC soil slope prior to the occurrence of major rainfall.

References

Aleotti, P. (2004). "A warning system for rainfall-induced shallow failures." Eng. Geology, 73, 247-265.

Au, S. W. C. (1998). "Rain-induced slope instability in Hong Kong." *Eng. Geology*, 51(1), 1-36.

Brand, E. W. (1984). "Landslides in Southeast Asia: A state-of-art report." *Proc., 4th Int. Symp. on Landslides,* Toronto, 17-59.

Brand, E. W. (1992). "Keynote Paper: Slope Instability in Tropical Areas." *Proc. 6th Int. Symp. on Landslides*, D. H. Bell, ed., Balkema, Rotterdam, The Netherlands, 2031-2051.

Cai, F. and Ugai, K. (2004). "Numerical analysis of rainfall effects on slope stability." *Int. J. of Geomech., ASCE,*4(2), 69-78.

Calvello, M., Cascini, L. and Sorbino, G. (2007). "A numerical procedure for predicting rainfall-induced movements of active landslides along pre-existing slip surfaces." *Int. J. for Numerical and Analytical Methods in Geomechanics*, 32(4), 327-351.

Chen, H., Lee, C. F. and Law, K. T. (2004). "Causative mechanisms of rainfall-induced fill slope failures." *J. of Geotech. and Geoenvironmen. Eng.*, 130(6) 593-602.

Ching, R. K. H. and Fredlund, D. G. (1984). "Quantitative comparison of limit equilibrium methods of slices." *Proc. 4th Int. Symp. on Landslides*. Toronto, Canada, 373-379.

Collins, B. D. and Dobroslav, Z. (2004). "Stability analyses of rainfall induced landslides." *J. of Geotech. and Geoenvironment. Eng.,* 130(4), 362-372.

Crosta, G. B. (2001). “Failure and flow development of a complex slide: The 1993 Sesa landslide.” *Eng. Geology*, 59(1-2), 173-199.

Fourie, A. B. (1996). “Predicting rainfall-induced slope instability.” *Proc. of the Inst. of Civil Eng. Geotech. Eng.*, 119(4) 211-218.

Frattini, P., Crosta, G. and Sosio, R. (2009). “Approaches for defining thresholds and return periods for rainfall-triggered shallow landslides.” *Hydrological Processes*, 23(10),1444-1460

Fredlund, D. G., Morgenstern, N. R. and Widger, R. A. (1978). “The shear strength of unsaturated soils.” *Canadian Geotechnical Journal*, 15(3), 313-321.

Fredlund, D. G. and Rahardjo, H. (1993). “Soil mechanics for unsaturated soils.” Wiley, New York

Fredlund, D. G. and Xing, A. Q. (1994). “Equations for the soil-water characteristic curve.” *Can. Geotech. J.*, 31(4), 533-546.

Geo-slope International, (2004a). *SEEP/W for finite element seepage analysis, version 4, user’s guide*, Calgary, Alta., Canada.

Geo-slope International, (2004b). *SLOPE/W for slope stability analysis*, *version 4, user’s guide*, Calgary, Alta., Canada.

Guzzetti, F., Peruccacci, S., Rossi, M. and Stark, C. P. (2007). “Rainfall thresholds for the initiation of landslides in central and southern Europe.” *Meteorology and Atmospheric Physics*, 98(3-4), 239-67.

Kim, J., Jeong, S., Park, S. and Sharma, J. (2004). “Influence of rainfall-induced wetting on the stability of slopes in weathered soils.” *Eng. Geology*, 75(3-4), 251-262.

Leong, E. C. and Rahardjo H. (1997). “Review of soil-water characteristic curve equations.” *J. of Geotech. and Geoenvironmental Eng.*, 123(12), 1106-1117.

McDougall, J., Ng, C. W. W. and Shi, Q. (1999). “Discussion of 'Influence of rainfall intensity and duration on slope stability in unsaturated soils.” *Quarterly J. of Eng. Geology and Hydrogeology*, 32(3), 303-303.

Ng, C. W. W., Wang, B. and Tung, Y. K. (2001). “Three-dimensional numerical investigations of groundwater responses in an unsaturated slope subjected to various rainfall patterns.” *Can. Geotech. J.*, 38(5), 1049-1062.

Pitts, J. (1984). “An Investigation of Slope Stability on the NTI Campus, Singapore.” *Applied Research Project RP1/83*, Singapore, Nanyang Technological Institute.

PUB (2000). “Geology of the Republic of Singapore.” *Public Works Department*, Singapore.

Rahardjo, H., Lim, T. T., Chang, M. F. and Fredlund, D. G. (1995). “Shear-strength characteristics of a residual soil.” *Can. Geotech. J.*, 32(1), 60-77.

Rahardjo, H., Li, X. W., Toll, D. G. and Leong, E. C. (2001). “The effect of antecedent rainfall on slope stability.” *Geotech. and Geologic. Eng.*, 19(3-4), 371-399.

Rahardjo, H., Ong, T. H., Rezaur, R. B. and Leong, E. C. (2007). “Factors controlling instability of homogeneous soil slopes under rainfall.” *J. of Geotech. and Geoenvironment. Eng.*, 133(12), 1532-1543.

Rahardjo, H., Leong, E. C. and Rezaur, R. B. (2008). "Effect of antecedent rainfall on pore-water pressure distribution characteristics in residual soil slopes under tropical rainfall." *Hydrological Processes*, 22(4) 506-523.

Rahardjo, H., Lee, T. T., Leong, E. C. and Rezaur, R. B. (2005). "Response of a residual soil slope to rainfall." *Can. Geotech. J.*, 42(2), 340-351.

Tan, S.B., Tan, S.L., Lim, T.L. and Yang, K.S. (1987). "Landslide Problems and Their Control in Singapore." *Proc. 9th Southeast Asian Geotechnical Conf. on Geomechanics in Tropical Soils*. Bangkok, Thailand.

Tohari, A., Nishigaki, M. and Komatsu, M. (2007). "Laboratory rainfall-induced slope failure with moisture content measurement." *J. of Geotech. and Geoenvironment. Eng.,* 133(5), 575-587.

Toll, D.G., Rahardjo, H. and Leong, E.C. (1999). "Landslides in Singapore." *2th Int. Conf. On Landslides, Slope Stability and the Safety of Infra-Structures*, Singapore.

Tsai, T. L., Chen, H. E. and Yang, J. C. (2008). "Numerical modeling of rainstorm-induced shallow landslides in saturated and unsaturated soils."" *Environmental Geology*, 55(6), 1269-1277.

Tsaparas, I., Rahardjo, H., Toll, D.G. and Leong, E.C. (2002). "Controlling parameters for rainfall-induced landslides." *Computers and Geotechnics*, 29(1), 1-27.

Wei, J., Heng, Y.S., Chow, W.C and Chong, M.K. (1991). "Landslides at Bukit Batok Sports Complex." *Proc. 9th Asian Conf on Soil Mechanics and Foundation Engineering*. Bangkok, Thailand, 445-448.

Yoshida, Y., Kuwano, J. and Kuwano, R. (1991). “Rain-induced slope failures caused by reduction in soil strength.” *Soils and Foundations*, 31(4), 187-193.

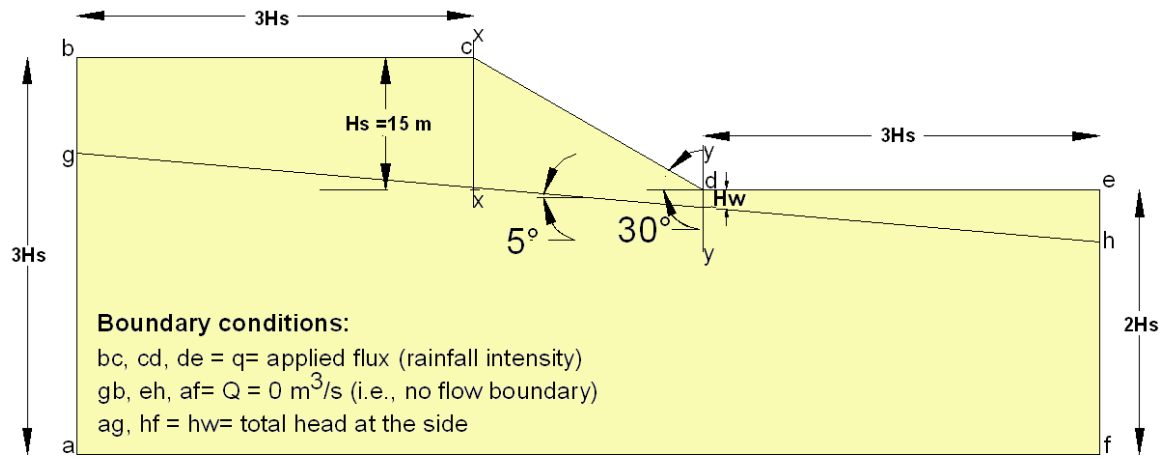

Fig.1. Slope geometry and boundary conditions for a homogeneous soil slope

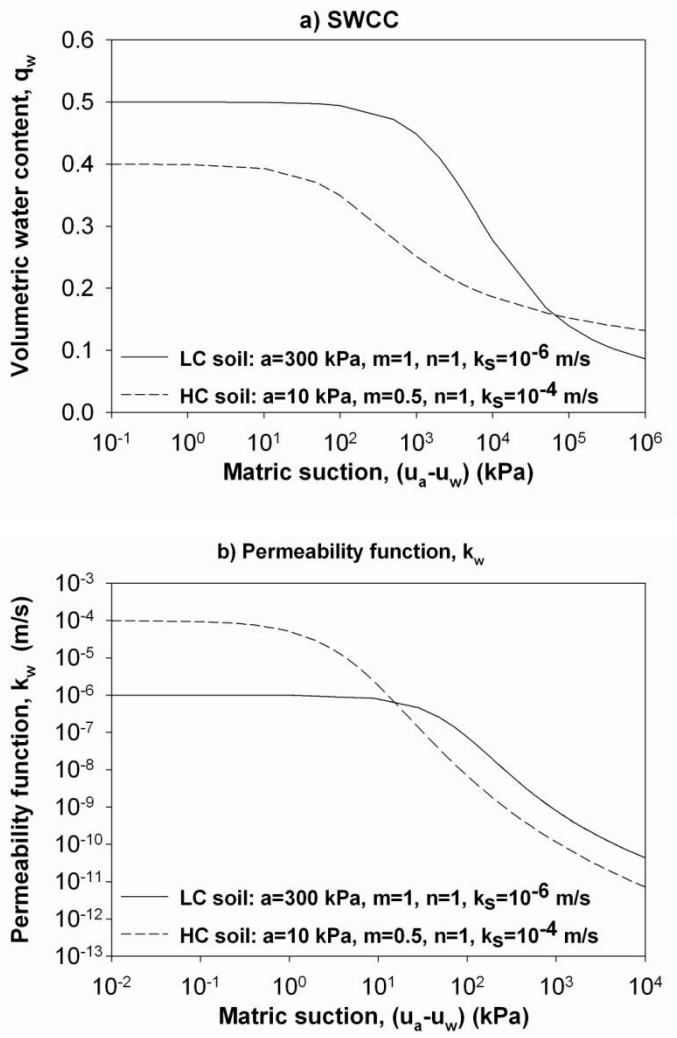

Fig.2. SWCC and unsaturated permeability function, k_w, of the HC and LC soil

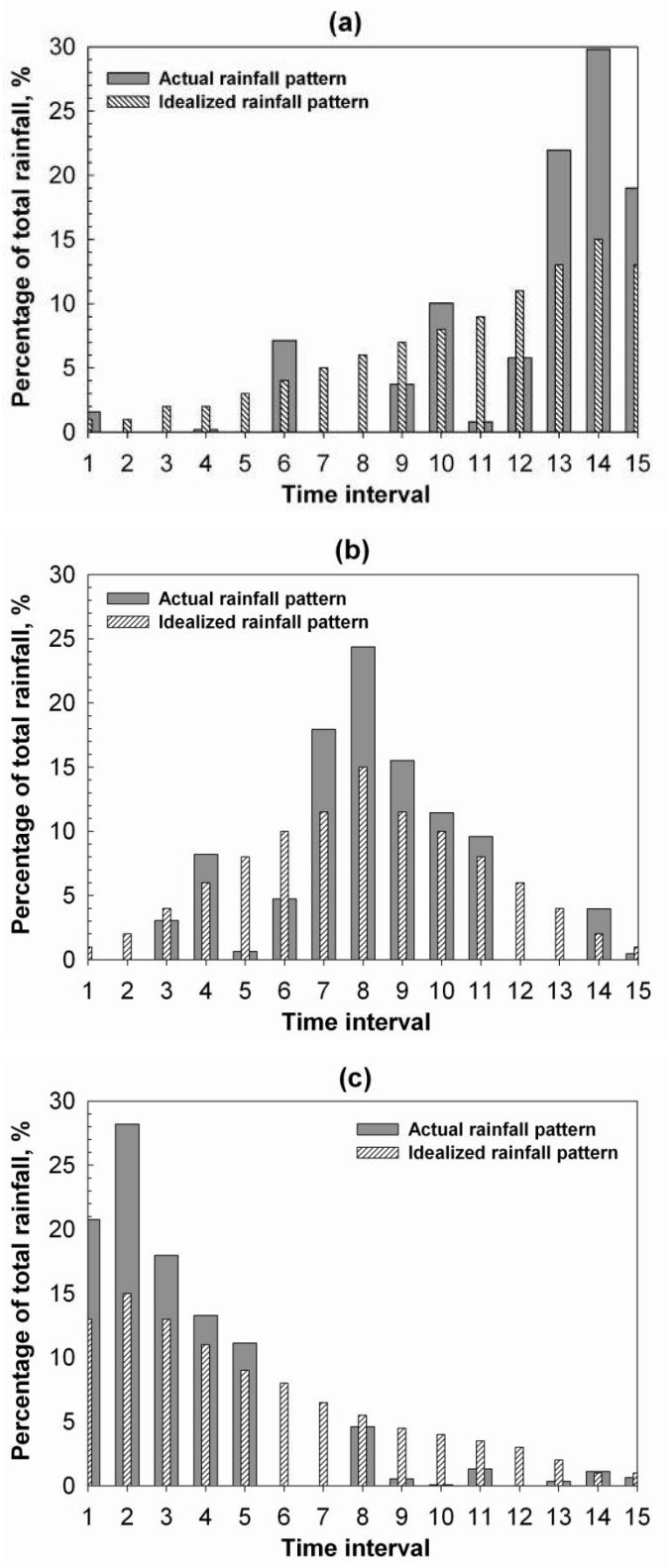

Fig.3. Actual and Idealized rainfall patterns for rainfall data of December 2006

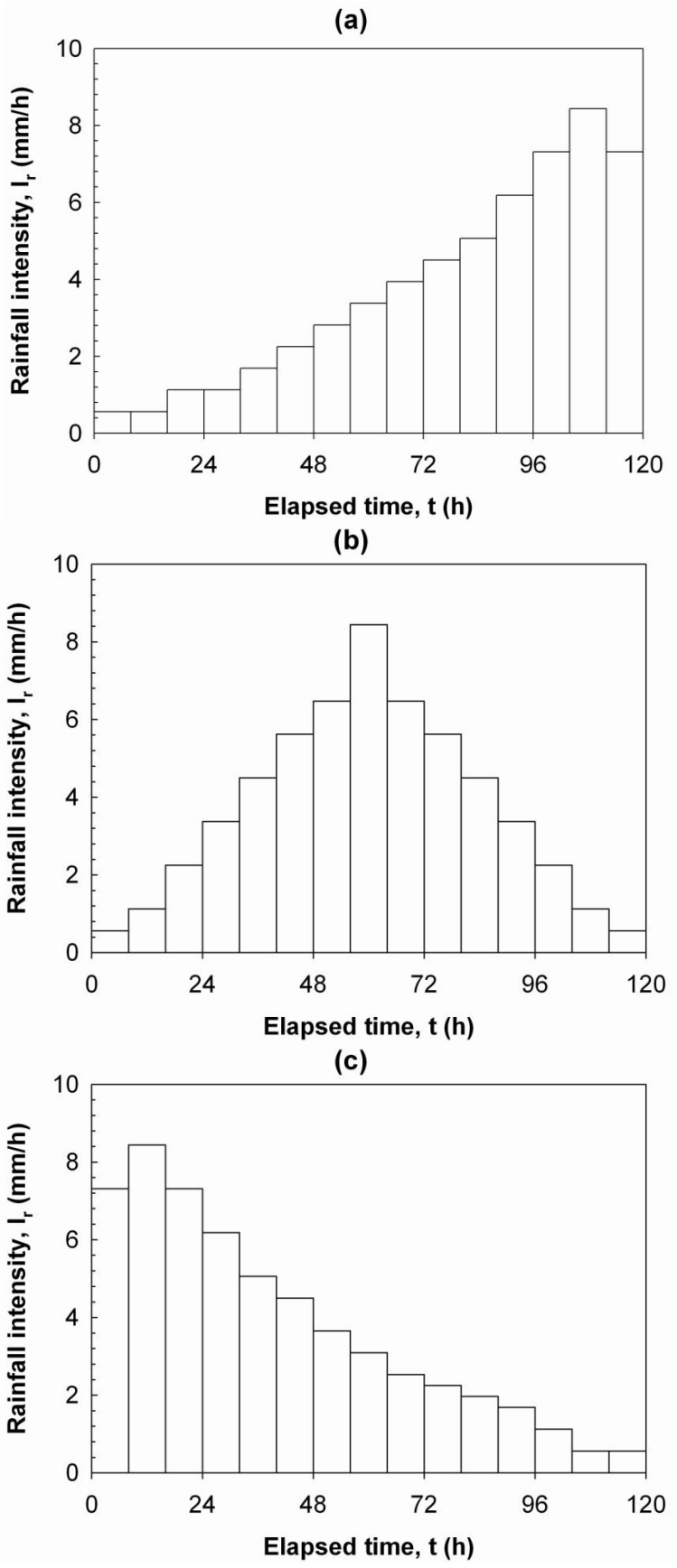

Fig.4. Designed rainfall patterns: a) Delayed rainfall pattern, b) Normal rainfall pattern, c) Advanced rainfall pattern

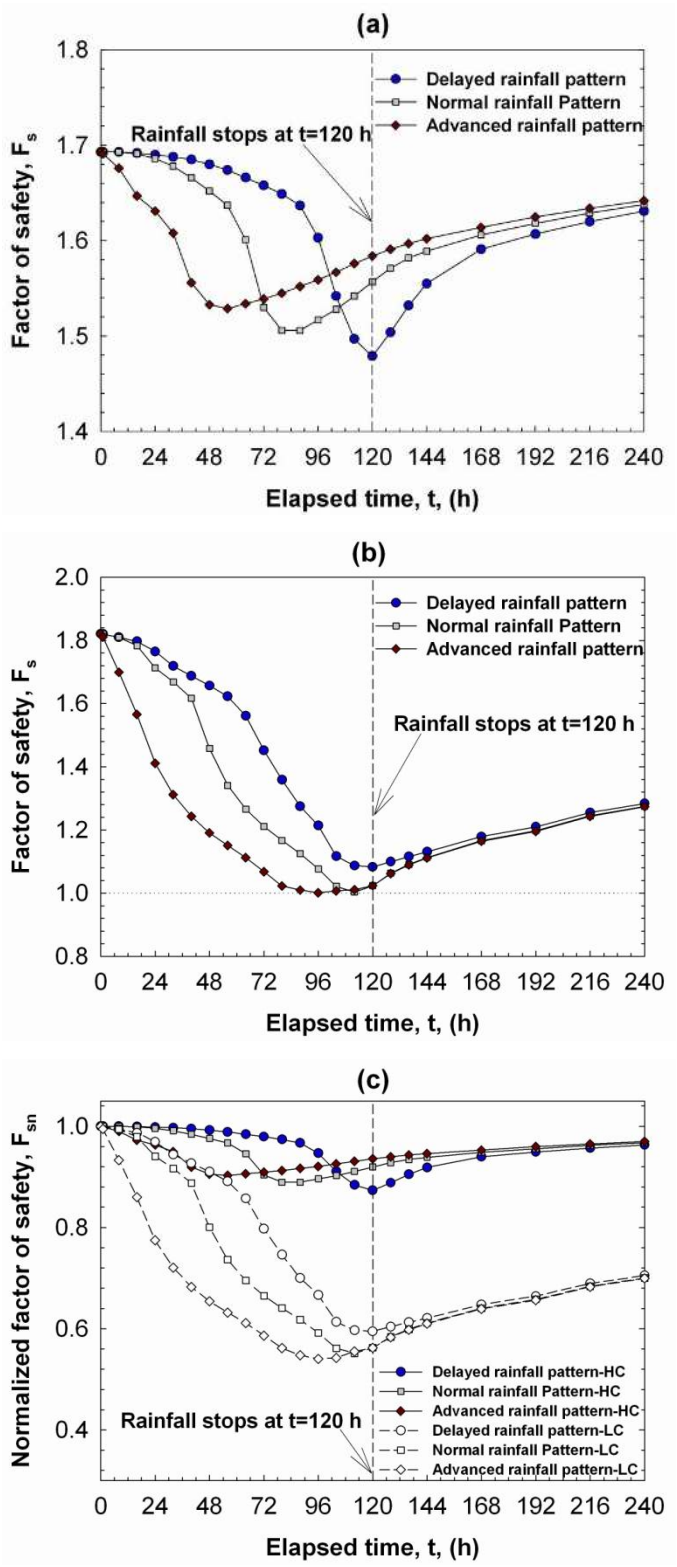

Fig.5. Normalized factor of safety, F_{sn}, versus time, t, for various rainfall patterns, a) HC soil type, b) LC soil type, c) comparison between HC and LC

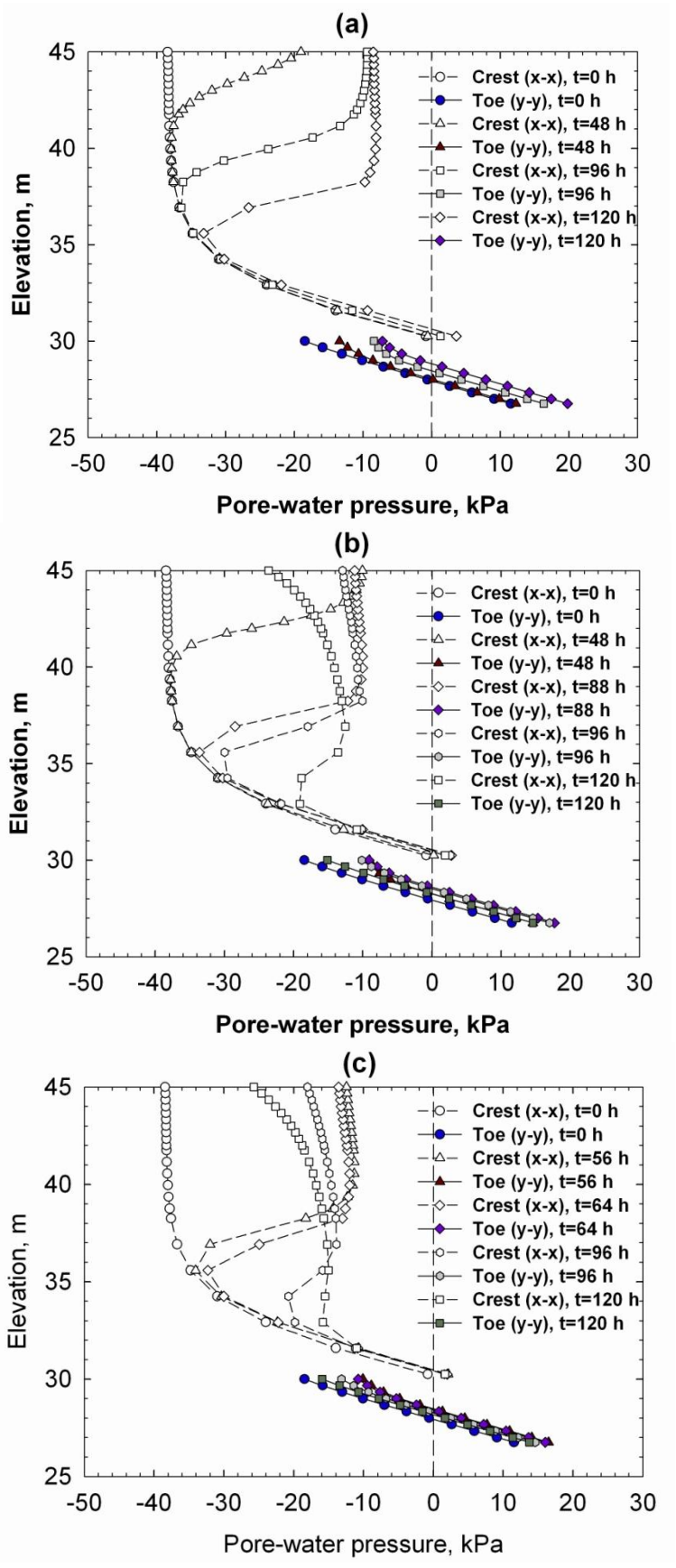

Fig.6. Pore-water pressure distribution caused by antecedent rainfall at crest (x-x) and toe (y-y) cross section for HC soil type, a) Delayed rainfall pattern, b) Normal rainfall pattern, c) Advanced rainfall pattern

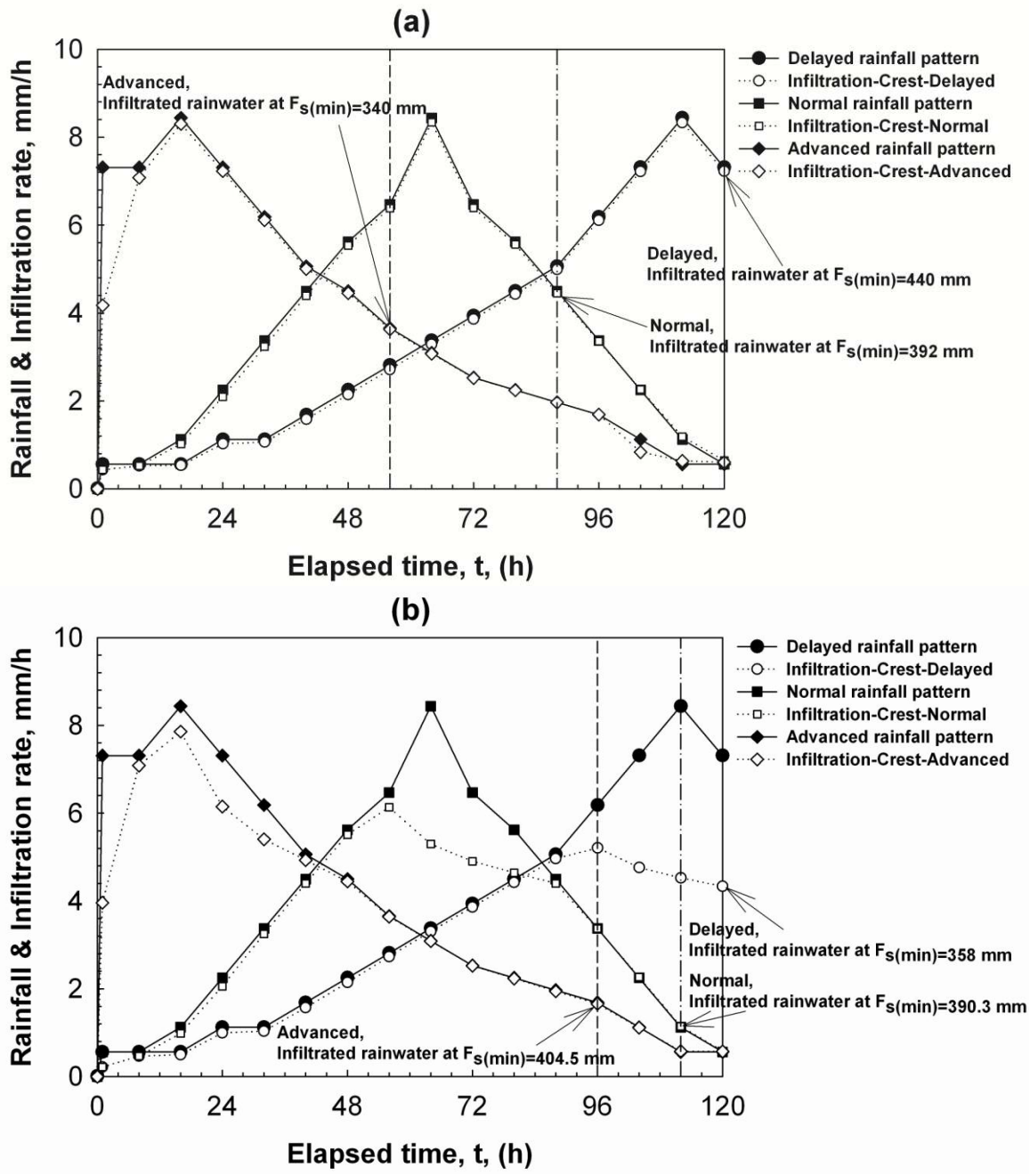

Fig.7. Rainfall and infiltration rate for antecedent rainfall patterns at crest of the slope a) HC soil slope b) LC soil slope

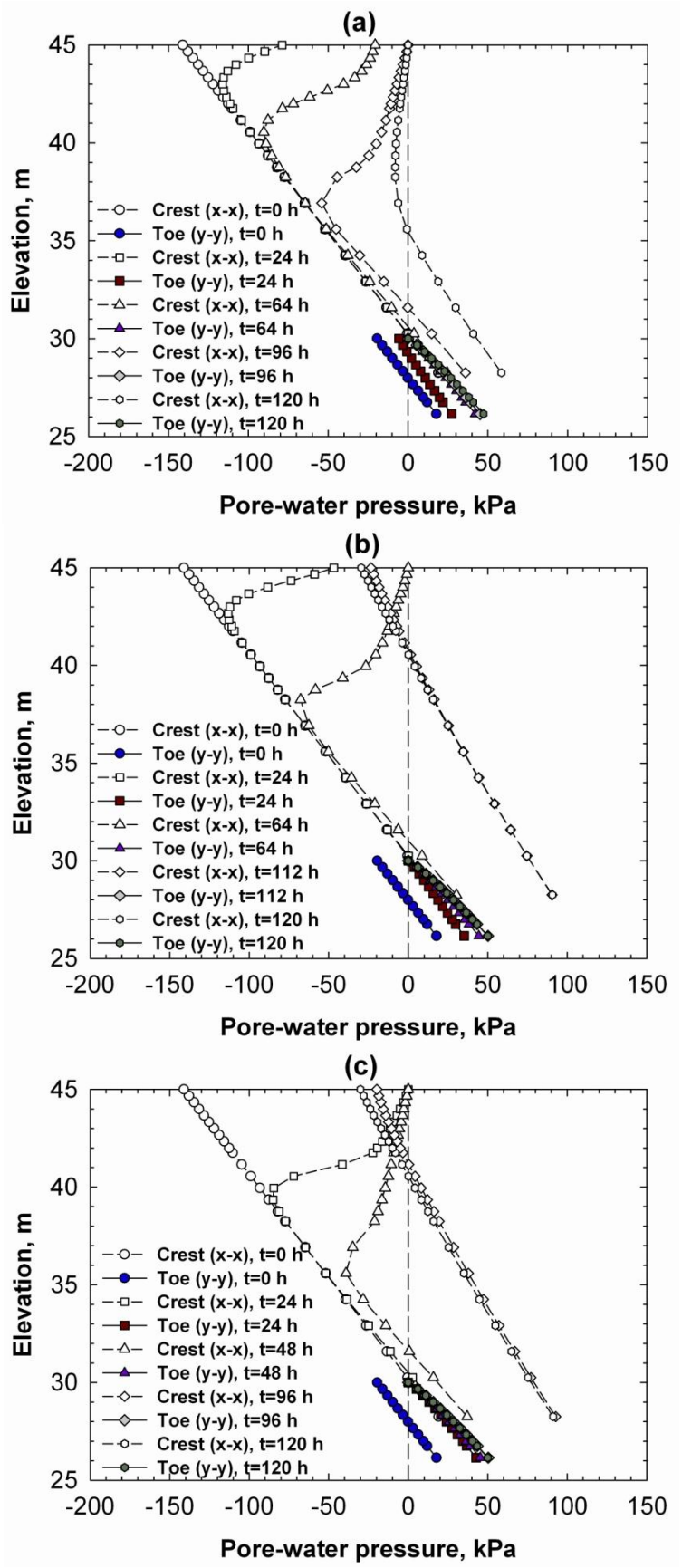

Fig.8. Pore-water pressure distribution caused by antecedent rainfall at crest (x-x) and toe (y-y) cross section for LC soil type, a) Delayed rainfall pattern, b) Normal rainfall pattern, c) Advanced rainfall pattern

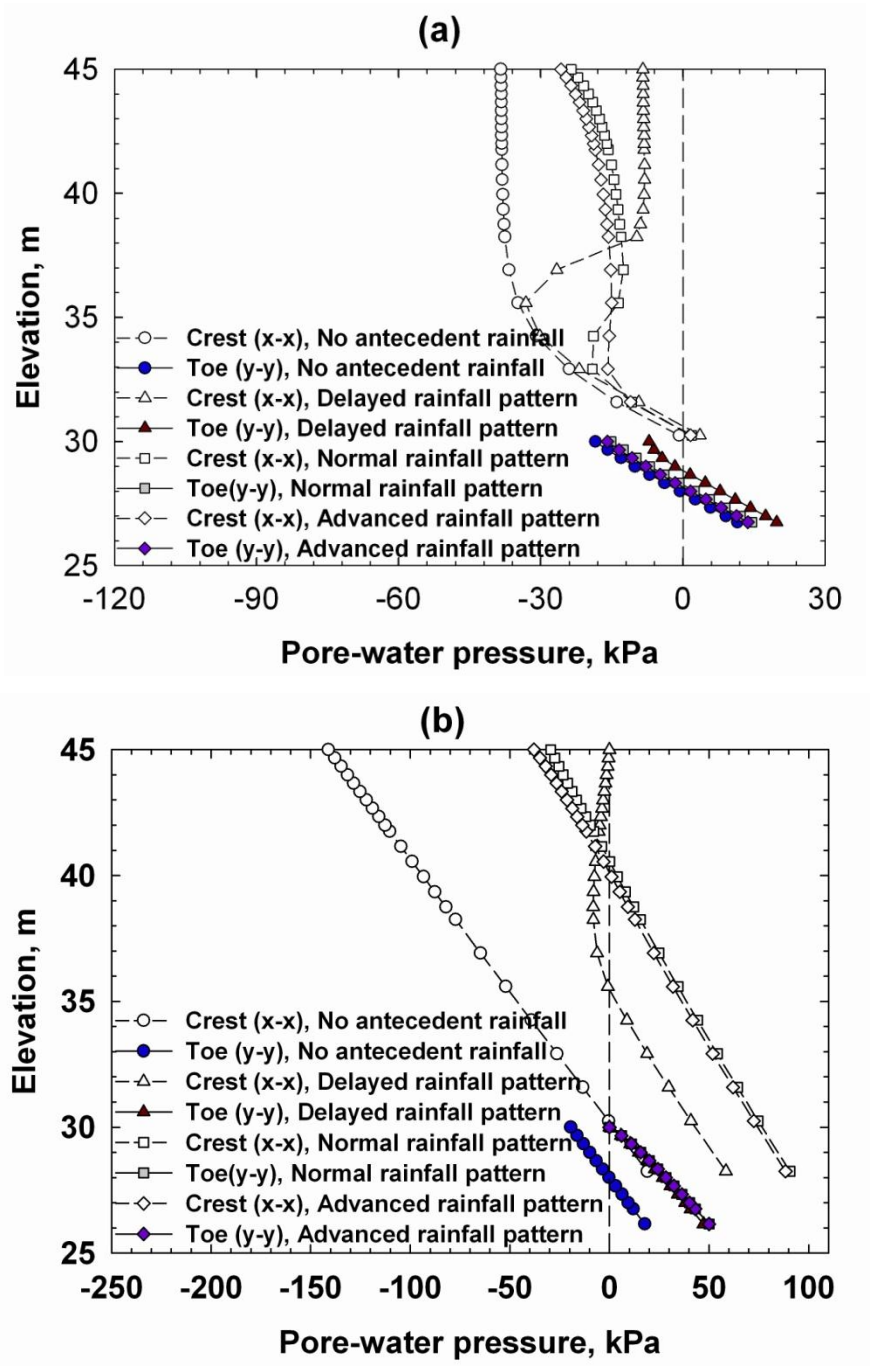

Fig.9. Initial conditions caused by antecedent rainfall patterns at the start of major rainfall, a) HC soil type, b) LC soil type

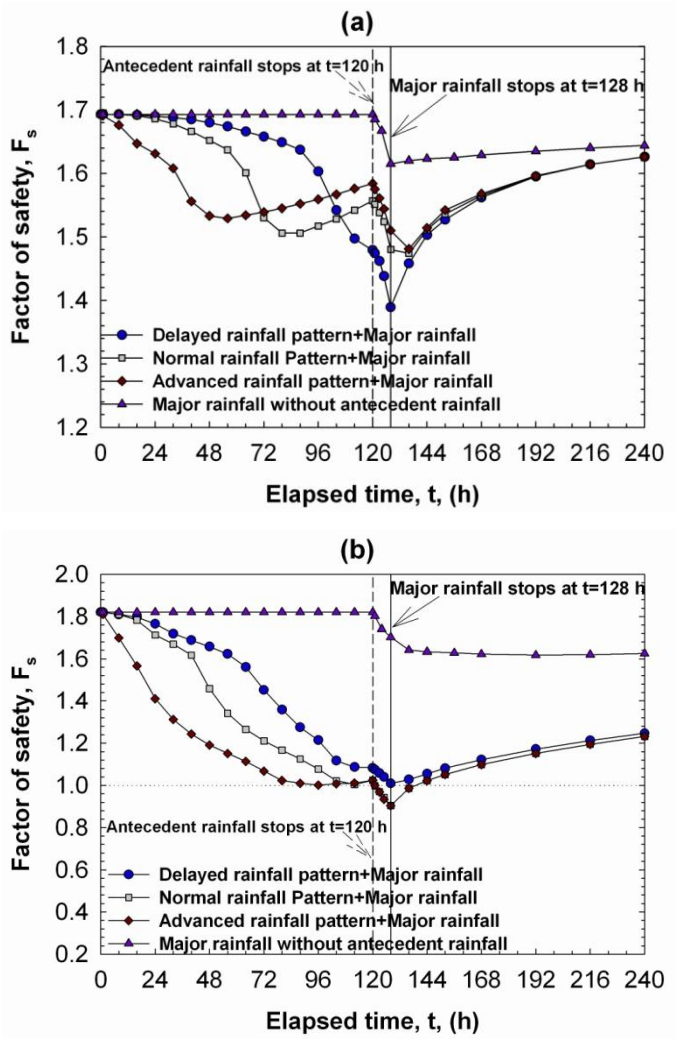

Fig.10. Factor of safety, Fs, versus time, t, for major rainfall with various initial conditions a) HC soil type, b) LC soil type